

# Registration and fusion of CT and SPECT images using mutual information

Lisa Tang<sup>†</sup>, Ghassan Hamarneh<sup>†</sup>, Anna Celler<sup>‡</sup>

<sup>†</sup> Department of Computing Sciences, SFU <sup>‡</sup> Department of Radiology, UBC

## Introduction

The goal of this research is to perform image registration of three-dimensional Single Photon Emission Computed Tomography (SPECT) and Computed Tomography (CT) images in a fast and accurate manner.

SPECT is a diagnostic technique that is based on the detection of radiation emitted by a tracer injected into the patient's body. While providing useful functional information, it has poor spatial resolution and often lacks anatomical landmarks necessary for the localization of organs. Conversely, computed tomography (CT) images provide rich anatomical information in high resolution but limited functional information. A fusion of CT and SPECT images would thus aid localizing regions of interests in the SPECT image. Additionally, once the CT and SPECT images are registered, corrections can be made on the SPECT images to improve their quantitative accuracy.

## Background

### Overview of Image Registration

Image registration is a process in which a series of spatial transformations  $T$  is being applied to one image  $m$  until it aligns with another image  $f$ . To evaluate how well the transformation has mapped  $m$  onto  $f$ , a similarity metric  $S(f, T(m))$  is used.

### Mutual Information

Common similarity metrics make assumptions about the pixel values of the images and become invalid when images are obtained from different imaging modalities. In contrast, the mutual information metric measures the statistical relationship between images and is thus applicable for CT-SPECT registrations [2,3].

Formally, the mutual information MI of images A and B is:

$$MI(A,B) = H(A) + H(B) - H(B,A)$$

where  $H(A)$  is the entropy of image A and  $H(B,A)$  is the joint entropy of A and B. Conceptually,  $H(A)$  describes the amount of uncertainty (information) an image contains and  $H(B,A)$  describes the amount of uncertainty about B when A is given [2]. The latter term is minimal when the images are aligned because this uncertainty is minimal when corresponding regions overlap. Thus, our task is to find  $T$  that would maximize  $MI(A, T(B))$ .

## Methods & Materials

### The Registration Procedure

The calculation of MI was based on the implementation by Mattes et al. [3]. We used the registration framework provided by the Insight ToolKit to execute the registration procedure as follows:

1. Resample the CT image ( $f$ ) so that its voxel size  $V_{size}$  is isotropic.
2. Apply an initial translation  $T = [x\ y\ z]$  to the SPECT image ( $m$ ) to align their centers of gravity.
3. Perform registration: **minimize** the **negative** value of MI over the search space defined by the transformation parameters using gradient-descent minimization scheme. Specifically, in each iteration:
  - Transform applies  $T$  to  $m$  to obtain  $m_T$ .
  - Interpolator calculates pixel intensities of  $m_T$  that are located at non-integral coordinates.
  - Metric calculate  $MI(f, m_T)$  that is parameterized by sample size  $N_{Samples}$  and number of bins  $N_{Bins}$ .
  - Optimizer advances the parameters of  $T$  with a maximum step size  $L_{Step}$  along the direction of  $\partial MI$  (the actual step size  $l$  is automatically computed using a bipartition scheme).
  - Iteration ends when  $l < L_{min}$ .

The entire pipeline is shown in Figure 1. Note the different parameters required at each stage. Table 1 outlines some of the parameters used in one registration trial.

To improve the accuracy and robustness of the algorithm, registration was performed in a coarse-to-fine manner [3, 4, 5]. To facilitate this, the input images were successively smoothed and down-sampled based on a *schedule* to form two image pyramids of coarse-to-fine resolutions.

Table 1. A subset of parameters of one registration trial

Level	XY reduction		Z reduction		# of Bins	# of Samples	Step size $L$	
	CT	SPECT	CT	SPECT			$L_{Step}$	$L_{Min}$
1	0.5	0.5	0.75	0.5	20	10000	4	0.1
2	0.75	0.75	0.5	0.75	20	20000	2	0.01
3	1	1	1	1	30	25000	1	0.001

At each level, the input images were down-sampled by the scale factors shown. Because of the anisotropic voxel size of the CT image, scaling in Z is less extreme. The maximum- and minimum- step size describes the rate of optimization and can be interpreted as the precision of the final transform.

### Materials – Patient data

In this study, three clinical data sets were used for the evaluation of the algorithm. Two came from pelvic bone studies and one from a thoracic study. Details of each type of data are specified in Table 1.

Table 2. Specifications of data sets

Studies	Resolution	Voxel Dimensions
Pelvic – CT	512 x 512 x 109	0.977 x 0.977 x 3
– SPECT	128 x 128 x 70	4.664 <sup>3</sup>
Thoracic – CT	512 x 512 x 125	0.650 x 0.650 x 3
– SPECT	128 x 128 x 78	4.664 <sup>3</sup>

Resolution (in pixels) and dimensions (in mm) of each image.

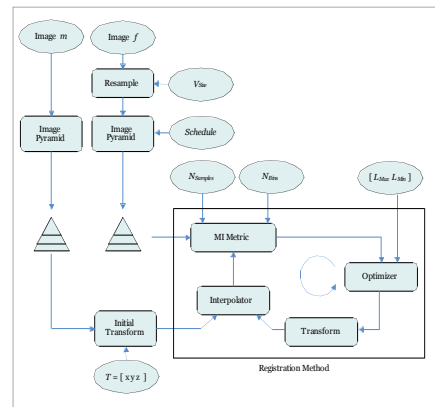


Figure 1. The basic components of our multi-resolution registration framework. The different parameters required by each component are drawn in ellipses.

## Results

### Results

The method was tested on the clinical data-sets described previously. To access the reproducibility of the various parameter combinations, we performed 24 separate trials for each set of data using different initial orientations and parameters. Numerical results are listed in Table 3.

Validation was done visually through 2D and 3D fusions (see figures below) and by observing the convergence in the MI similarity metric and the translation parameters (see Discussion).

Table 3. Registration results

Study	Mean translation parameters (in mm)			Mean MI
	X	Y	Z	
Pelvic1	44.537 ± 0.391	51.522 ± 0.838	9.619 ± 0.071	-0.052
Pelvic2	45.423 ± 0.398	53.107 ± 0.312	9.47 ± 1.221	-0.091
Thorax	119.580 ± 0.611	133.318 ± 0.991	6.980 ± 1.941	-0.098

In each trial, the final translation in X-, Y-, Z- dimensions and metric value are recorded. The differences are calculated by averaging the difference of each calculated translation to the mean translation.

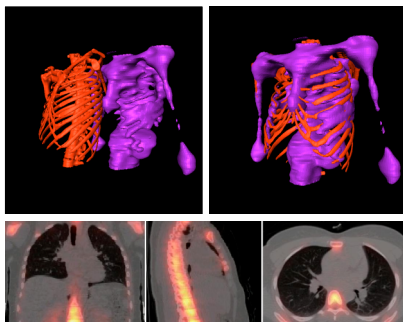


Figure 2. Top left: the 3D fusion of CT and SPECT images from the thoracic study created before registration. The red skeletal structure was generated from the original CT 3D image; the purple from SPECT. Top right: 3D fusion created after registration. Below row: 2D fusions of the registered images shown in coronal, sagittal and axial views (CT image in grey and SPECT in red).

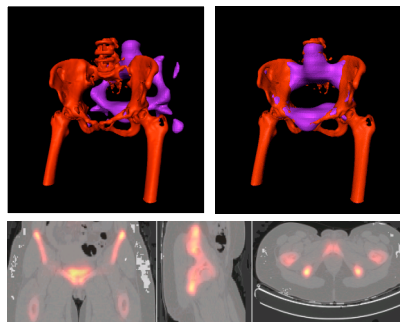


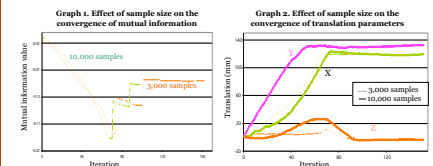
Figure 3. Top left: 3D fusion of the pelvic study created before registration. The red skeletal structure generated from CT image; the purple from SPECT image. Top right: 3D fusion created after registration. Below: 2D fusion after registration (CT drawn in grey and SPECT in red).

## Discussions

One challenge of this research is to find the right set of parameters for each study. A useful approach is to analyze how the transformation parameters calculated by the algorithm and the metric value converge (examples are shown in charts below).

Some important observations were made on...

- **Sample size.** Too few samples would hamper the smoothness of the metric calculation while too many samples would result in a longer computation time (see graphs below). Our experiments indicate that 10,000 samples are sufficient for both types of study.
- **Initial alignment.** It is crucial when multi-resolution is not used but it is not needed when multi-resolution is used.
- **Multi-resolution levels.** A balance is needed between computation time and registration quality. A 3-level registration on average took 6 minutes to initialize while a 4-level took 9 minutes. Conversely, registration would fail when too few levels were used because the optimization might be trapped in local minima.



The graphs illustrate how the metric value and translation parameters changed after each iteration and compare the results of using different sample sizes. In Graph 2, the change in X-, Y-, Z- translations when 3,000 samples (solid line) and 10,000 samples (dotted) are used.

## Conclusions

Medical image registration is of importance for diagnosis and medical research. Particularly, the registration of CT and SPECT images has allowed for not only the attenuation correction of SPECT images but also eased the localization of the regions of interest they captured. In this research, the use of mutual information has shown to be an effective and accurate similarity criterion for the registration of CT and SPECT images in thoracic and pelvic studies. The multi-resolution approach also helped increase the likelihood of entrapment in local minima. Future work can be directed at performing non-rigid registration on these images.

### References

- [1] J. Pluim, A. Maintz and M. Viergever, "Mutual information based registration of medical images: a survey," *IEEE Trans. Med. Imag.*, vol. 21, pp. 61-75, 2003.
- [2] L. Ibáñez, W. Schroeder, and the Insight Consortium. *The ITK software Guide*. The Insight Consortium, Feb 2003. <http://www.itk.org/>
- [3] W. M. Wells, P. Viola, H. Atsumi, S. Nakajima, R. Kikinis, "Multi-modal volume registration by maximization of mutual information," *Med. Imag. Analysis*, vol. 1, pp. 53-61, 1996.
- [4] P. J. Slomka, D. Dey, C. Przetak, U. E. Aladi, R. P. Baum, "Automated 3-Dimensional registration of stand-alone <sup>18</sup>F-FDG whole-body PET with CT," *J. of Nuclear Med.*, vol. 44(7), July 2003.